

Removal of Heavy Metals from Aqueous Systems with Thiol Functionalized Superparamagnetic Nanoparticles

WASSANA YANTASEE,^{*,†}
 CYNTHIA L. WARNER,[†]
 THANAPON SANGVANICH,[‡]
 R. SHANE ADDLEMAN,[†]
 TIMOTHY G. CARTER,[§]
 ROBERT J. WIACEK,[†] GLEN E. FRYXELL,[†]
 CHARLES TIMCHALK,[†] AND
 MARVIN G. WARNER^{*,†}

Pacific Northwest National Laboratory, Richland, Washington 99352, Department of Chemical Engineering, Chulalongkorn University, Bangkok, Thailand, and Department of Chemistry, University of Oregon, Eugene, Oregon 97403

We have shown that superparamagnetic iron oxide (Fe₃O₄) nanoparticles with a surface functionalization of dimercaptosuccinic acid (DMSA) are an effective sorbent material for toxic soft metals such as Hg, Ag, Pb, Cd, and Tl, which effectively bind to the DMSA ligands and for As, which binds to the iron oxide lattices. The nanoparticles are highly dispersible and stable in solutions, have a large surface area (114 m²/g), and have a high functional group content (1.8 mmol thiols/g). They are attracted to a magnetic field and can be separated from solution within a minute with a 1.2 T magnet. The chemical affinity, capacity, kinetics, and stability of the magnetic nanoparticles were compared to those of conventional resin based sorbents (GT-73), activated carbon, and nanoporous silica (SAMMS) of similar surface chemistries in river water, groundwater, seawater, and human blood and plasma. DMSA-Fe₃O₄ had a capacity of 227 mg of Hg/g, a 30-fold larger value than GT-73. The nanoparticles removed 99 wt % of 1 mg/L Pb within a minute, while it took over 10 and 120 min for Chelex-100 and GT-73 to remove 96% of Pb.

Introduction

The removal of heavy metals, such as mercury, lead, thallium, cadmium, and arsenic, from natural waters has attracted considerable attention because of their adverse effects on environmental and human health. Enhancement of sorbent materials into nanoporous structures has shown to significantly improve their performance in metal removal when compared to conventional sorbent beds (1–3). However, such nanomaterials still suffer from issues involving mass transport of large water volumes through the materials. A dispersible sorbent with a large surface area and suitable chemistry would be very advantageous for the removal of heavy metals from aqueous solutions.

* Address correspondence to either author. Phone: (509)376-1728 (W.Y.); (509)376-0834 (M.G.W.). E-mail: wassana.yantasee@pnl.gov (W.Y.); marvin.warner@pnl.gov (M.G.W.).

[†] Pacific Northwest National Laboratory.

[‡] Chulalongkorn University.

[§] University of Oregon.

Iron oxide nanoparticles are highly dispersible in solutions. With particle sizes of less than 40 nm, they offer a large surface area and superparamagnetic properties; they are attracted to a magnetic field but do not retain magnetic properties when the field is removed (4), making them highly useful in novel separation processes. Specifically, unmodified maghemite (γ -Fe₂O₃) was reported for successful capturing of Cr(VI) (5), while magnetite (Fe₃O₄) nanoparticles modified with an oleic acid ligand were reported for capturing As(III) and As(V) (6, 7), both by exploiting a strong reactivity between iron oxides and metal species. Attachment of undecanoic acid on γ -Fe₂O₃ nanoparticles (8) and chitosan on Fe₃O₄ nanoparticles (9) resulted in magnetic sorbent materials effective for the capture of Cd and Cu, respectively.

In this work, iron oxide (Fe₃O₄) nanoparticles were functionalized with dimercaptosuccinic acid (DMSA) to create a novel dispersible sorbent that can be magnetically collected and has a high capacity and selectivity for the softer heavy metals. Liquid DMSA has been recognized as an excellent chelating agent for heavy metals and is approved by the FDA for the treatment of Hg and Pb poisoning (10). Modification of the nanoparticle surface with DMSA was anticipated to increase the efficacy of the magnetic nanoparticles for heavy metal removal. Although the DMSA modified iron oxide nanoparticles have been studied for medical imaging (11–14), this is the first time that their use as magnetic sorbent materials for soft heavy metals has been reported. Along with the DMSA-Fe₃O₄ nanoparticles, three commercial sorbents, including Duolite GT-73 resins, Chelex-100 resin, Darco KB-B activated carbon, and PNNL's patented self-assembled thiol monolayer on a mesoporous support (SH-SAMMS) (15, 16) were also tested for comparison.

Experimental Procedures

Synthesis of Nanoparticles. Syntheses of bare Fe₃O₄ and DMSA-Fe₃O₄ were modified from previous reports (17, 18) and described in the Supporting Information.

Batch Metal Sorption. Metal sorption equilibrium and kinetics were performed on the DMSA-Fe₃O₄ in batch experiments (see the Supporting Information for experimental procedures and matrices).

Distribution Coefficient (K_d) Measurements. Sorbent performance was frequently evaluated with the distribution coefficient (K_d) (in mL/g), which is simply a mass-weighted partition coefficient between liquid supernatant phase and solid phase as follows:

$$K_d = \frac{(C_o - C_f) V}{C_f M} \quad (1)$$

where C_o and C_f are the initial and final concentrations in the solution of the target species determined by ICP-MS, V is the solution volume in milliliters, and M is the mass in grams of the sorbent.

Results and Discussion

The interaction of the ligand with the iron oxide surface is either a hydrogen bonding interaction through the OH group (under acidic conditions) or a direct Fe-carboxylate linkage (at more alkaline pH values as in this study) (19). See Figure 1 in the Supporting Information for graphical representation of DMSA-Fe₃O₄. The surface properties, metal sorption capabilities, and stability of the DMSA modified Fe₃O₄ nanoparticles were systematically evaluated, and results are reported herein.

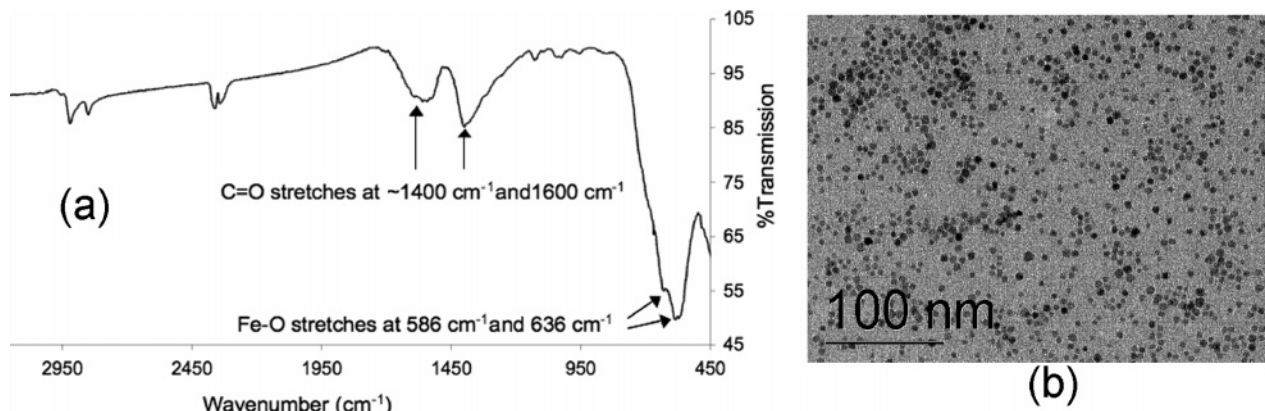


FIGURE 1. (a) IR spectrum and (b) TEM image of DMSA modified Fe_3O_4 .

Surface Properties. Detailed surface characterization of DMSA- Fe_3O_4 is presented in the Supporting Information. Successful surface modification with DMSA moieties was verified with infrared spectroscopic analysis of the material as shown in Figure 1a. In the IR spectrum, the C=O stretches were found at ~ 1400 and 1600 cm^{-1} , and the S-H stretches were found at 2345 and 2370 cm^{-1} , which are typically very weak and convoluted by contamination of the CO_2 stretching bands from the background (20). The fact that we observe the carboxylate stretches at 1600 and 1400 cm^{-1} is consistent with the carboxylate anion interacting with the FeO surface since the free carboxylic acid would have a C=O stretch above 1700 cm^{-1} (21). Also, the fact that an S-H stretch is observed is consistent with the free thiol and not a surface bound metal thiolate (21). The frequency of the thiol S-H stretch is unusual (ca. 2400 cm^{-1} , as opposed to about 2550 cm^{-1} for a normal thiol), but this is presumably due to thiol aggregation within the monolayer and hydrogen bonding effects. Other previous work (22) also suggested that it is the carboxylate and not the thiol that is bound to the FeO surface.

BET analysis revealed a surface area of $114\text{ m}^2/\text{g}$. TEM images (Figure 1b) of nanoparticles prepared in an aqueous system revealed an average particle size of $5.8 \pm 0.9\text{ nm}$ with little to no evidence of large aggregate formation. Elemental analysis of S and Fe indicated that 1 g of the DMSA- Fe_3O_4 nanoparticles contained $0.80 \pm 0.03\text{ g}$ ($3.5 \pm 0.1\text{ mmol}$) of Fe_3O_4 and $0.16 \pm 0.01\text{ g}$ ($0.91 \pm 0.05\text{ mmol}$) of DMSA (or 1.82 mmol of thiols). A change in water solubility from completely insoluble to fully water soluble was observed upon binding of the DMSA ligands to the surface of the originally hydrophobic nanoparticles, suggesting full or nearly full replacement of lauric acid by the incoming DMSA ligands. This was supported by our calculations. By assuming a footprint of about 20 \AA^2 per DMSA molecule (a lower boundary value based on a footprint of closely packed carboxylic acids at the Fe_3O_4 interface (23)) on the nanoparticles with a surface area of $114\text{ m}^2/\text{g}$, a fully dense monolayer coverage would contain $14.7\text{ wt } \%$ DMSA and $85.3\text{ wt } \%$ Fe_3O_4 . Thus, the observed value of $16\text{ wt } \%$ DMSA suggested nearly full monolayer coverage on these particles.

Magnetic Collection of DMSA- Fe_3O_4 . Discussion of the particle size dependence of the magnetic collection of Fe_3O_4 nanoparticles has been reported (7). As a balance between surface area, stability, magnetic collectability, and ease of synthesis, we chose to work with 6 nm particles. At this particle size, it can be observed in all cases that magnetic removal of the nanoparticles from the liquid phase was as nearly effective, yet faster than centrifugation (see Table 3 in Supporting Information). At an L/S ratio of 10^4 , only 2% of the nanoparticles was left in the solution after 1 min of magnetic separation. The ability to remove the nanoparticles of this small size from the liquid phase with a relatively low

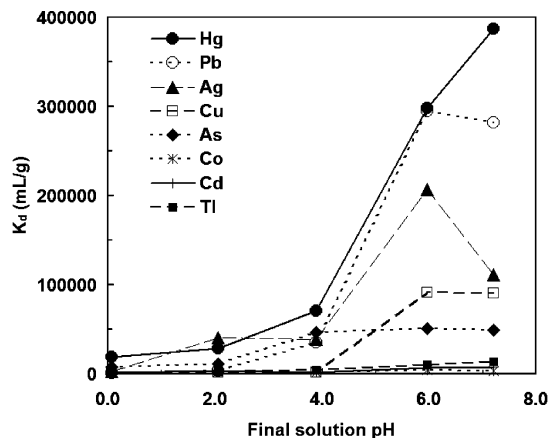


FIGURE 2. Effect of pH on the K_d values, measured in HNO_3 spiked unfiltered river water (L/S, 10^5).

magnetic field gradient suggests that the nanoparticles formed aggregates under the applied field gradient (7). This aggregation is believed to be reversible once the field is removed (7); thus, the nanoparticles have the advantages of high surface area and magnetic collectability under a reasonable field gradient.

Metal Sorption Properties. The chemical binding affinity of a sorbent can be expressed in terms of the distribution coefficient (K_d). The higher the K_d value, the more effective the sorbent material is at capturing and holding the target species. In general, K_d values of $\sim 10^3\text{ mL/g}$ are considered good, and those above 10^4 mL/g are outstanding (24). The K_d values were measured and evaluated as a function of sample pH, differing matrices, L/S ratio, and on differing sorbents.

Chemical Affinity as a Function of Sample pH. The ability of a sorbent material to remove a metal ion depends on the $\text{p}K_a$ of its ligand, the stability constant of the metal-ligand complex, the presence of competitive ligands in solution, the pH of the solution (25), and the metals ions' capacity to undergo hydrolysis (26). Figure 2 shows the binding affinity (K_d) of DMSA- Fe_3O_4 to various metal ions in HNO_3 spiked unfiltered river water. As anticipated from Pearson's hard-soft acid-base theory (HSAB) (27), soft ligands like the thiol groups in DMSA prefer to bind soft metals like Hg and Ag, rather than a relatively harder metal such as Co. From the K_d values, the DMSA- Fe_3O_4 nanoparticles are an outstanding sorbent for Hg, Ag, Pb, Cu, and As ($K_d > 50,000\text{ mL/g}$) and a good sorbent for Cd, Co, and Tl in river water at neutral pH.

From Figure 2, the binding affinities of all metals were higher in neutral river water than in HNO_3 spiked river water. This is because when the pH of the water was lower than the

TABLE 1. K_d of DMSA-Fe₃O₄ Nanoparticles in Differing Matrices for Selected Metals

matrix	pH	L/S	cobalt	copper	silver	cadmium	mercury	thallium	lead
0.025 M NaNO ₃	3.46	10 ⁵	2300	1600	800	2600	1 100 000	3800	9200
0.025 M NaAc	4.71	10 ⁵	1400	680	11 000	2800	510 000	3600	22 000
0.025 M PBS	7.33	10 ⁵	7500	21 000	10 000	9900	29 000	5500	24 000
unfiltered river water	7.20	10 ⁵	3200	91 000	110 000	7400	390 000	13 000	280 000
unfiltered ground water	7.77	10 ⁵	6800	63 000	58 000	12 000	420 000	11 000	110 000
unfiltered sea water	7.64	10 ⁵	4100	170 000	2800	2200	16 000	2300	570 000
human plasma	8.01	10 ⁴							120 000
human blood	7.41	10 ⁴							12 000

pK_a of DMSA ($pK_{a,COOH}$ of 2.71 and 3.43 and $pK_{a,SH}$ of 9.65 (28)), the functional groups remain protonated, thereby reducing affinities at lower pH values. However, it should be noted that large K_d values above 10⁴ can still be observed in the lower pH ranges. It is also possible that the observed pH dependent adsorption of different metal ions is significantly impacted by the capacity of metal ions to undergo hydrolysis and second by an ion's water exchange rate and ease of forming a new, stable complex (26). The retention of high K_d values until highly acidic conditions suggests that the DMSA-Fe₃O₄ nanoparticles are suitable for direct disposal of stabilized, concentrated toxic metals. At above pH 7, a noticeable drop in the K_d value of Ag may be a result of a strong association between Ag(I) and reduced sulfur groups in organic matter (e.g., in bacterial or algal cells and humic substances) (29) often found in river water.

Matrix Effect on K_d . In natural water samples, competitive complexation of metal ions with water constituents (e.g., inorganic and organic ligands) limit the interaction between the metal species and the sorbent. Other metal ions present in the nonideal solutions may also compete for the binding sites. Constituents of natural waters, such as suspended organics, may clog the pores of the sorbent materials. Therefore, the K_d value and other sorption properties should be evaluated in the same or similar matrices in which the sorbent materials are intended for use. Table 1 summarizes the K_d values of multiple metal ions on DMSA-Fe₃O₄ in different matrices. As expected from the pH isotherm (Figure 2), Hg binding on DMSA-Fe₃O₄ was less affected in low pH matrices (e.g., pH 3.6) than Pb binding. Anions (nitrate, acetate, and phosphate) impacted the K_d value of metal ions in different manners. In all natural fresh waters, the binding affinity of DMSA-Fe₃O₄ to Pb, Hg, Cu, and Ag was outstanding. In contrast, the binding of Hg and Ag in seawater was less efficient due to their known complexation with chloride ions (prevalent in seawater) to form negatively charged complexes (e.g., HgCl₃⁻, HgCl₄²⁻, AgCl₃²⁻, and AgCl₂⁻ (30, 31)), which do not bind favorably to DMSA. In plasma, the K_d value of Pb was similar to that in unfiltered groundwater but 10-fold higher than that in human blood, suggesting that red blood cell constituents (mainly hemoglobin) competed with the nanoparticles for Pb (32). Regardless, the K_d value on the order of 10⁴ to 10⁵ suggests that the nanoparticles may potentially be a new alternative chelating agent for Pb that offers an advantage over the FDA-approved liquid DMSA because they may be cleared directly from blood and plasma by bypassing the kidney with an applied magnetic field.

K_d as a Function of L/S. Table 2 shows the effect of L/S on the K_d values of Pb on DMSA-Fe₃O₄ nanoparticles in various matrices. In solutions containing nitrate (NaNO₃), acetate (NaAc), and phosphate buffered saline (PBS), increasing the L/S ratio from 10⁵ to 5 × 10⁵ clearly increased the K_d value of Pb, suggesting that the binding sites were not yet saturated at a L/S ratio of 10⁵. However, in unfiltered river water containing organic matter, while increasing the L/S ratio from 10⁴ to 10⁵ clearly provides an improvement in the K_d value, further increases in the L/S ratio from 10⁵ to

TABLE 2. Effect of Liquid to Solid Ratio (L/S) on K_d of Pb with DMSA-Fe₃O₄

matrix	L/S (mL/g)	K_d (mL/g) of Pb
0.025 M NaNO ₃ , pH 3.46	1 × 10 ⁵	9200
	5 × 10 ⁵	25 000
0.025 M NaAC, pH 4.71	1 × 10 ⁵	22 000
	5 × 10 ⁵	280 000
0.025 M PBS, pH 7.33	1 × 10 ⁵	2400
	5 × 10 ⁵	110 000
unfiltered river water, pH 7.20	1 × 10 ⁴	5100
	1 × 10 ⁵	110 000
	1 × 10 ⁶	130 000

10⁶ did not significantly increase the K_d value of Pb. At higher L/S ratios, the inhibition of the binding of Pb to the DMSA-Fe₃O₄ nanoparticles may be caused by the interaction between Pb and river water constituents, thus preventing it from binding to the nanoparticles.

K_d Comparison Against Other Sorbents. Table 3 summarizes the K_d values of metal ions measured on different sorbents containing thiols. Note that thallium was added into the solutions as Tl⁺ and arsenic as As(III). In terms of the K_d values, DMSA-Fe₃O₄ is significantly superior to commercial GT-73 and activated carbon (Darco KB-B) for capturing Hg, Cd, Ag, Pb, and Tl. The affinity of DMSA-Fe₃O₄ for As was more modest than for other metals and similar to that on unmodified Fe₃O₄, which is indicative that the DMSA ligand shell has very little impact upon As capture. This supports the irreversible adsorption of As onto the core material previously reported (7). Nevertheless, the massive improvement in K_d values clearly shows the excellent utilization of the DMSA ligand shell. When compared to the commercial sorbents tested, both DMSA-Fe₃O₄ and SH-SAMMS are outstanding sorbents for Pb, Hg, Cd, Cu, and Ag. However, being superparamagnetic, the DMSA-Fe₃O₄ nanoparticles have the unique capability of being magnetically manipulated.

Sorption Capacity. Figure 3 shows the adsorption isotherms of Hg on DMSA-Fe₃O₄, SH-SAMMS, and GT-73 in filtered groundwater (pH 8.1). The isotherm curves present the Hg uptake as a function of the equilibrium Hg solution concentration at room temperature. Apparent Hg precipitation in groundwater at high Hg concentrations was observed by substantial deviation from Langmuirian adsorption. Therefore, for the isotherm measurements, the Hg concentrations in the starting solutions were kept below 5 mg/L, and the lowest practical mass of sorbent per solution ratio (L/S of 5 × 10⁵ for DMSA-Fe₃O₄ and SH-SAMMS and 7000 for GT-73) was used to ensure a very large excess of Hg per binding capacity of each material to achieve the saturation sorption. Hg removal by the sorbents was then normalized by the mass of the sorbent materials used. The Langmuir parameters derived from the linear regression (see eqs 1 and 2 in the Supporting Information) of the Hg adsorption isotherm data on the three sorbents in filtered groundwater are presented in Table 2 of the Supporting Information. The

TABLE 3. K_d (mL/g) of Metal Ions on Selected Sorbents in Ground Water^a

sorbent	final pH	colbalt	copper	arsenic	silver	cadmium	mercury	thallium	lead
DMSA-Fe ₃ O ₄	6.91	3000	270 000	5400	3 600 000	10 000	92 000	14 000	2 300 000
Fe ₃ O ₄	6.93	1600	7400	5800	13 000	2400	16 000	4000	78 000
SH-SAMMS	6.80	430	1 700 000	950	67 000 000	66 000	1 100 000	15 000	350 000
GT-73	6.76	890	6300	1200	16 000	1500	10 000	2200	41 000
Darco KB-B	6.90	790	26 000	750	27 000	1300	31 000	21	190 000

^a L/S = 10 000 mL/g in 0.45 μm filtered groundwater.

TABLE 4. Stability of DMSA-Fe₃O₄ in Differing Fluids^a

matrix	mg Fe release per g of DMSA-Fe ₃ O ₄	% Fe dissolved per total Fe
deionized water	1.6 ± 0.6	0
HNO ₃ spiked groundwater, pH 3.2	1.4 ± 0.0	0
HNO ₃ spiked river water, pH 2	8.1 ± 0.0	1
0.1 M HNO ₃	18 ± 3	3
0.5 M HCl	29 ± 2	5
1.0 M HNO ₃	67 ± 7	11
5.0 M HNO ₃	620 ± 88	100
5.0 M HCl	633 ± 87	100
2.0 M NaOH	28 ± 11	4
human plasma	0.2 ± 0.1	0

^a All measured in duplicates, L/S = 100 000 mL/g.

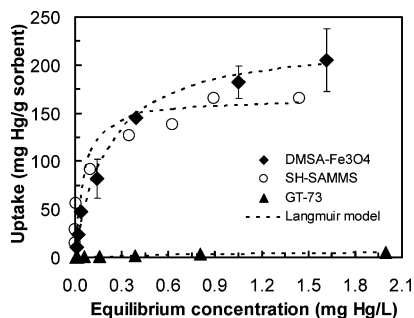


FIGURE 3. Adsorption isotherm of Hg in groundwater (pH 8.1) on DMSA-Fe₃O₄ (L/S, 5 × 10⁵), SH-SAMMS (L/S, 5 × 10⁵), and GT-73 (L/S, 7000). Dashed lines represent Langmuir modeling of the data.

good agreement between the data and the Langmuir adsorption model (all linear fit correlations, $R^2 > 0.98$) implies that the adsorption of Hg onto the three materials occurred as a single monolayer and was uniformly distributed across the sorbent surface, not nucleating or precipitating out of solution.

The large surface area of DMSA-Fe₃O₄ (114 m²/g) and SH-SAMMS (74 m²/g) afforded a high number of ligands on the materials, leading to a large ion loading capacity. The maximum Hg sorption capacity of DMSA-Fe₃O₄ was 227 mg of Hg/g (0.010 mmol of Hg/m²), which was comparable to that of SH-SAMMS (measured to be 167 mg of Hg/g or 0.011 mmol of Hg/m² in this matrix) but 30-fold larger than that of GT-73 (8 mg of Hg/g or 0.001 mmol of Hg/m²). This was expected since as shown in Table 3 both DMSA-Fe₃O₄ and SH-SAMMS had a much higher binding affinity (K_d) for Hg in filtered groundwater than did GT-73. Although the capacity of GT-73 for Hg in deionized water (pH 4–6) was reported to be 600 mg/g (33), the measured Hg capacity in groundwater reported here is only 8 mg/g, which suggests very poor utilization of the GT-73 binding sites in groundwater. At maximum sorption, the molar ratio of Hg per DMSA was approximately 1:1, suggesting that the DMSA binding sites spread uniformly on the surface of nanoparticles and were fully accessible to bind with the metal ion (5).

Sorption Kinetics. In addition to sorption affinity, capacity, and selectivity to the target metal ions, it is important

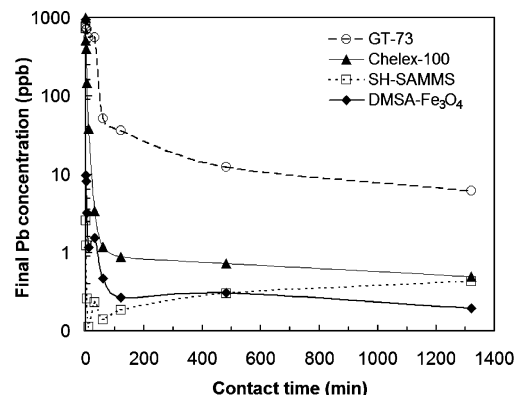


FIGURE 4. Kinetics of adsorption of 1000 ppb Pb in filtered groundwater, pH 7.77, all with L/S of 1000, except DMSA-Fe₃O₄ with L/S of 2000.

that a sorbent material offers rapid sorption to minimize the time required to remove metal ions. Figure 4 shows the uptake rate of Pb on various sorbent materials measured in filtered groundwater (pH 7.7). Even with half the mass of sorbent per solution volume (L/S of 2000), DMSA-Fe₃O₄ could remove Pb as well as SH-SAMMS and better than the two commercial sorbents, Chelex-100 and GT-73 (L/S of 1000). Specifically, after 1 min of contact time, over 99 wt % of 1 mg/L Pb was removed with DMSA-Fe₃O₄ and SH-SAMMS, while only 48 and 9 wt % of Pb was removed with Chelex-100 and GT-73, respectively. It took over 10 and 120 min for Chelex-100 and GT-73 to remove over 96% of Pb. GT-73 and Chelex-100 are created by attaching ligands on porous polymer resins; thus, they often suffer from solvent swelling and have dendritic porosities. SH-SAMMS has a rigid silica support and open pore structure that allow for rapid diffusion of analytes into the binding sites, resulting in extremely fast sorption kinetics. Likewise, the accessibility of metal ions to the binding sites can be readily achieved at DMSA-Fe₃O₄ nanoparticles having DMSA ligands coated on the exterior surface. The absence of internal diffusion resistance of the nanoparticles leads to the sorption kinetics that was observed to be as rapid as those on SH-SAMMS.

Material Stability and Digestibility. The stability of DMSA-Fe₃O₄ materials in the solution phase was assessed

by the extent of the Fe leachate into the solution phase per gram of the material after contacting it for 2 h with various fluids as shown in Table 4. DMSA-Fe₃O₄ was relatively stable (leachate <5 wt % of total Fe) in matrices ranging from 0.5 M acid solution to a strong alkaline solution (2.0 M NaOH), suggesting that they can be used in most natural and wastewaters. Leachate of Fe from the nanoparticles also was not observed in human plasma, suggesting that the material may be used in biological matrices as a heavy metal decorporating agent. The Fe leachate also was not affected by the type of acid (e.g., HNO₃ vs HCl); thus, the instability of the material in acid was due to ligand protonation and not the oxidation metal center. The counterions (nitrate vs chloride) had little impact on the stability. Digestion of metal bound magnetic nanoparticles to recover the metals would be very easy (e.g., in 5 M acid at room temperature). The same approach was previously performed (34) on GT-73 in an attempt to release preconcentrated metals for analytical determination but was found to be problematic as digestion of the GT-73 substrate was found to be difficult.

Acknowledgments

This work was supported by a Project BioShield grant from NIAID, Grant 1R21 OH008900-01 from NIOSH, and the PNNL's LDRD. Its contents are solely the responsibility of the authors and do not necessarily represent the official views of the NIH. T.G.C. gratefully acknowledges the NSF. This research was performed in part at the Environmental Molecular Sciences Laboratory (EMSL), a DOE national scientific user facility located at PNNL. The authors thank Dr. Joongjai Panpranot, Dr. Cynthia Bruckner-Lea, Dr. Karla Thrall, Cynthia Dutton, Dean Moore, and Jolen Soelberg for their contributions.

Supporting Information Available

Synthesis methods for bare Fe₃O₄ and DMSA modified Fe₃O₄, surface characterization of the nanoparticles, batch contact protocols, ICP-MS operating conditions, linear Langmuir isotherm parameters, and magnetic collectability of the nanoparticles. This material is available free of charge via the Internet at <http://pubs.acs.org>.

Literature Cited

- (1) Fryxell, G. E.; Liu, J.; Mattigod, S. V.; Wang, L. Q.; Gong, M.; Hauser, T. A.; Lin, Y.; Ferris, K. F.; Feng, X. Environmental issues and waste management technologies in the ceramic and nuclear industries, environmental applications of interfacially modified mesoporous ceramics. In *Ceramics Transactions*; Chandler, G. T., Feng, X., Eds.; The American Ceramic Society: Westerville, OH, 2000; Vol. 107, pp 29–37.
- (2) Fryxell, G. E.; Lin, Y.; Wu, H.; Kemner, K. M. Environmental applications of self-assembled monolayers on mesoporous supports (SAMMS). In *Studies in Surface Science and Catalysis*; Sayari, A., Jaroniec, M., Eds.; Elsevier Science: Amsterdam, 2002; Vol. 141, pp 583–590.
- (3) Fryxell, G. E.; Addleman, R. S.; Mattigod, S. V.; Lin, Y.; Zemanian, T. S.; Wu, H.; Birnbaum, J. C.; Liu, J.; Feng, X. *Environmental and Sensing Applications of Molecular Self-Assembly*; Marcel-Dekker: New York, 2004.
- (4) O'Handley, R. C. *Modern Magnetic Materials. Principles and Applications*; John Wiley and Sons: New York, 2000.
- (5) Hu, J.; Chen, G.; Lo, I. M. C. Removal and recovery of Cr(VI) from wastewater by maghemite nanoparticles. *Water Res.* **2005**, *39*, 4528–4536.
- (6) Yavuz, C. T.; Mayo, J. T.; Yu, W. W.; Prakash, A.; Falkner, J. C.; Yean, S.; Cong, L.; Shipley, H. J.; Kan, A.; Tomson, M.; Natelson, D.; Colvin, V. L. *Science* **2006**, supporting online material; www.sciencemag.org/cgi/content/full/314/5801/5964/DC5801.
- (7) Yavuz, C. T.; Mayo, J. T.; Yu, W. W.; Prakash, A.; Falkner, J. C.; Yean, S.; Cong, L.; Shipley, H. J.; Kan, A.; Tomson, M.; Natelson, D.; Colvin, V. L. Low-field magnetic separation of monodisperse Fe₃O₄ nanocrystals. *Science* **2006**, *314*, 964–967.

- (8) Hai, B.; Wu, J.; Chen, X.; Protasiewicz, J. D.; Scherson, D. A. Metal-ion adsorption on carboxyl-bearing self-assembled monolayers covalently bound to magnetic nanoparticles. *Langmuir* **2005**, *21*, 3104–3105.
- (9) Chang, Y.-C.; Chen, D.-H. Preparation and adsorption properties of monodisperse chitosan-bound Fe₃O₄ magnetic nanoparticles for removal of Cu(II) ions. *J. Colloid Interface Sci.* **2005**, *283*, 446–451.
- (10) Miller, A. L. Dimercaptosuccinic acid (DMSA), A non-toxic, water-soluble treatment for heavy metal toxicity. *Alt. Med. Rev.* **1998**, *3*, 199–207.
- (11) Lee, J.-H.; Huh, Y.-M.; Jun, Y.-w.; Seo, J.-w.; Jang, J.-t.; Song, H.-T.; Kim, S.; Cho, E.-J.; Yoon, H.-G.; Suh, J.-S.; Cheon, J. Artificially engineered magnetic nanoparticles for ultra-sensitive molecular imaging. *Nat. Med.* **2006**, *13*, 95–99.
- (12) Chaves, S. B.; Lacava, L. M.; Lacava, Z. G. M.; Silva, O.; Pelegrini, F.; Buske, N.; Gansau, C.; Morais, P. C.; Azevedo, R. B. Light microscopy and magnetic resonance characterization of a DMSA-coated magnetic fluid in mice. *IEEE Trans. Magn.* **2002**, *38*, 3231–3233.
- (13) Rivière, C.; Boudghène, F. P.; Gazeau, F.; Roger, J.; Pons, J.-N.; Laissy, J.-P.; Allaire, E.; Michel, J.-B.; Letourneur, D.; Deux, J.-F. Iron oxide nanoparticle-labeled rat smooth muscle cells: Cardiac MR imaging for cell graft monitoring and quantitation. *Radiology* **2005**, *235*, 959–967.
- (14) Bertorelle, F.; Wilhelm, C.; Roger, J.; Gazeau, F.; Menager, C.; Cabuil, V. Fluorescence-modified superparamagnetic nanoparticles: Intracellular uptake and use in cellular imaging. *Langmuir* **2006**, *22*, 5385–5391.
- (15) Feng, X. D.; Fryxell, G. E.; Wang, L. Q.; Kim, A. Y.; Liu, J.; Kemner, K. Functionalized monolayers on ordered mesoporous supports. *Science* **1997**, *276*, 923–926.
- (16) Chen, X. B.; Feng, X. D.; Liu, J.; Fryxell, G. E.; Gong, M. Mercury separation and immobilization using self-assembled monolayers on mesoporous supports (SAMMS). *Sep. Sci. Technol.* **1999**, *34*, 1121–1132.
- (17) Massart, R. Preparation of aqueous magnetic liquids in alkaline and acidic media. *IEEE Trans. Magn.* **1981**, *27*, 1247–1248.
- (18) Sun, S.; Zeng, H. Size-controlled synthesis of magnetite nanoparticles. *J. Am. Chem. Soc.* **2002**, *124*, 8204–8205.
- (19) Ulman, A. *An Introduction to Ultrathin Organic Films, from Langmuir-Blodgett to Self-Assembly*; Academic Press: San Diego, 1991; pp 239–245.
- (20) Jun, Y.-W.; Huh, Y.-M.; Choi, J.-S.; Lee, J.-H.; Song, H.-T.; Kim, S. J.; Yoon, S.; Kim, K.-S.; Shin, J.-S.; Suh, J.-S.; Cheon, J. Nanoscale size effect of magnetic nanocrystals and their utilization for cancer diagnosis via magnetic resonance imaging (MRI). *J. Am. Chem. Soc.* **2005**, *127*, Supporting Information p S5.
- (21) Silverstein, R. M.; Bassler, G. C.; Morrill, T. C. *Spectroscopic Identification of Organic Compounds*, 3rd ed.; John Wiley and Sons: New York, 1974.
- (22) Liu, Q.; Xu, Z. Self-assembled monolayer coatings on nanosized magnetic particles using 16-mercaptohexadecanoic acid. *Langmuir* **1995**, *11*, 4617–4622.
- (23) Shen, L. F.; Laibinis, P. E.; Hatton, T. A. Bilayer surfactant stabilized magnetic fluids: Synthesis and interactions at interfaces. *Langmuir* **1999**, *15*, 447–453.
- (24) Fryxell, G. E.; Lin, Y.; Fiskum, S.; Birnbaum, J. C.; Wu, H.; Kemner, K.; Kelly, S. Actinide sequestration using self-assembled monolayers on mesoporous supports. *Environ. Sci. Technol.* **2005**, *39*, 1324–1331.
- (25) Mellor, D. P. *Chemistry of Chelation and Chelating Agents*; Pergamon Press: New York, 1979.
- (26) Richens, D. T. *The Chemistry of Aqua Ions*; John Wiley and Sons: New York, 1997.
- (27) Pearson, R. G. Hard and soft acids and bases. *J. Am. Chem. Soc.* **1963**, *85*, 3533–3539.
- (28) Crisponi, G.; Diaz, A.; Nurchi, V. M.; Pivetta, T.; Tapia, Estevez, M. J. Equilibrium study on Cd(II) and Zn(II) chelates of mercaptocarboxylic acids. *Polyhedron* **2002**, *21*, 1319.
- (29) Herrin, R. T.; Andren, A. W.; Shafer, M. M.; Armstrong, D. E. Determination of silver speciation in natural waters. 2. Binding strength of silver ligands in surface freshwaters. *Environ. Sci. Technol.* **2001**, *35*, 1959–1966.
- (30) Powell, K. J.; Brown, P. L.; Byrne, R. H.; Gajda, T.; Hefter, G.; Sjöberg, S.; Wanner, H. Chemical speciation of Hg(II) with environmental inorganic ligands. *Aus. J. Chem.* **2004**, *57*, 993–1000.
- (31) Byrne, R. H. Inorganic speciation of dissolved elements in seawater: The influence of pH on concentration ratios. *Geochem. Trans.* **2002**, *3*, 11–16.

- (32) Simons, T. J. Passive transport and binding of lead by human red blood cells. *J. Physiol.* **1986**, *378*, 267–286.
- (33) Lloyd-Jones, P. J.; Rangel-Mendez, J. R.; Streat, M. Mercury sorption from aqueous solution by chelating ion exchange resin, activated carbon, and biosorbent. *Trans. IChemE, Part B: Process Safety Environ. Protect.* **2004**, *82*, 301–331.
- (34) Pohl, P.; Prusisz, B. On the applicability of Duolite GT-73 to column preconcentration of gold and palladium prior to

determination by inductively coupled plasma atomic emission spectrometry. *Microchim. Acta* **2005**, *150*, 159–165.

Received for review March 1, 2007. Revised manuscript received May 1, 2007. Accepted May 4, 2007.

ES0705238